

# CAT<sub>3</sub>, a prodrug of 13a(S)-3-hydroxyl-6,7-dimethoxyphenanthro[9,10-b]-indolizidine, circumvents temozolomide-resistant glioblastoma via the Hedgehog signaling pathway, independently of O<sup>6</sup>-methylguanine DNA methyltransferase expression

Ming Ji<sup>1</sup>  
Liyuan Wang<sup>1</sup>  
Ju Chen<sup>1</sup>  
Nina Xue<sup>2</sup>  
Chunyang Wang<sup>2</sup>  
Fangfang Lai<sup>2</sup>  
Rubing Wang<sup>1</sup>  
Shishan Yu<sup>1</sup>  
Jing Jin<sup>1,2</sup>  
Xiaoguang Chen<sup>1,2</sup>

<sup>1</sup>State Key Laboratory of Bioactive Substances and Functions of Natural Medicines, Institute of Materia Medica, Chinese Academy of Medical Sciences and Peking Union Medical College, Beijing 100050, People's Republic of China; <sup>2</sup>Beijing Key Laboratory of New Drug Mechanisms and Pharmacological Evaluation Study, Institute of Materia Medica, Chinese Academy of Medical Sciences and Peking Union Medical College, Beijing 100050, People's Republic of China

Correspondence: Jing Jin; Xiaoguang Chen  
Institute of Materia Medica, Chinese Academy of Medical Sciences and Peking Union Medical College, 1 Xiannongtan Street, Xicheng District, Beijing 100050, People's Republic of China  
Tel +86 10 6316 5207  
Email rebeccagold@imm.ac.cn;  
chxg@imm.ac.cn

**Purpose:** Glioblastoma multiforme (GBM) is a malignant high-grade glioma with a poor clinical outcome. Temozolomide (TMZ) is the first-line GBM chemotherapy; however, patients commonly develop resistance to its effects.

**Materials and methods:** We investigated the antitumor activity of CAT<sub>3</sub> in TMZ-resistant glioblastoma cell lines U251/TMZ and T98G. Orthotopic and subcutaneous mice tumor models were used to investigate the effects of various treatment regimes.

**Results:** We found that PF403, the active metabolite of CAT<sub>3</sub>, inhibited proliferation of both cell lines. PF403 repressed the Hedgehog signaling pathway in the U251/TMZ cell line, reduced O<sup>6</sup>-methylguanine DNA methyltransferase (MGMT) expression, and abolished the effects of the Shh pathway. Moreover, PF403 blocked the Hedgehog signaling pathway in T98G MGMT-expressing cells and downregulated the expression of MGMT. CAT<sub>3</sub> suppressed growth in the U251/TMZ orthotopic and T98G subcutaneous xenograft tumor models in vivo. We also demonstrated that inhibition of the Hedgehog pathway by PF403 counteracted TMZ resistance and enhanced the antitumor activity of TMZ in vitro and in vivo.

**Conclusion:** These results indicate that CAT<sub>3</sub> is a potential therapeutic agent for TMZ-resistant GBM.

**Keywords:** Gli inhibitor, chemotherapy, lomeguatrib, xenograft tumor model

## Introduction

Glioblastoma multiforme (GBM) is the most common and lethal malignant brain tumor, with a poor clinical outcome.<sup>1</sup> Based on the National Institutes of Health's The Cancer Genome Atlas (TCGA), numerous factors are considered to contribute to the development of GBM; these include the amplification of *EGFR*; mutation of *PIK3CA*, *IDH1*, and *EGFRvIII*; deletion of *PTEN*; and aberrations in the Hedgehog signaling pathway.<sup>2-4</sup> Among these factors, the Hedgehog signaling pathway has attracted the most attention recently owing to its potential utility as a therapeutic target. This signaling pathway is triggered by the interaction between the sonic Hedgehog (Shh) ligand and the receptor patched 1 (Ptch1), which blocks the activation of smoothened (Smo). After releasing the "brake effect" of Ptch1 against Smo, the transcriptional factor Gli

translocates into the nucleus and activates the expression of target genes.<sup>5</sup> Inhibition of the Hedgehog signaling pathway by vismodegib (GDC-0449) has been clinically indicated for advanced basal cell carcinoma driven by the abnormal Hedgehog pathway.<sup>6,7</sup> The Hedgehog signaling pathway is now considered a novel target for GBM treatment.<sup>8,9</sup>

According to the National Comprehensive Cancer Network guidelines, the alkylating agent temozolomide (TMZ) has shown favorable efficacy against and is considered first-line chemotherapy for GBM.<sup>10</sup> However, the acquisition of resistance to TMZ is common among patients, thereby reducing its clinical efficacy. Numerous factors are involved in TMZ resistance, such as O<sup>6</sup>-methylguanine DNA methyltransferase (MGMT), p-glycoprotein, and Gli.<sup>11–13</sup> The protein MGMT is an important determinant of TMZ resistance: the expression pattern of MGMT is reportedly associated with TMZ efficacy, and the methylation status of the *MGMT* promoter has been monitored as a clinical biomarker for GBM outcomes.<sup>14–16</sup>

CAT<sub>3</sub> is a prodrug of 13a(S)-3-hydroxyl-6,7-dimethoxyphenanthro[9,10-b]-indolizidine (PF403).<sup>17</sup> CAT<sub>3</sub> exerts potent antitumor activity in brain tumors, including glioblastoma and medulloblastoma, *in vivo*. Its metabolite, PF403, is capable of penetrating the blood–brain barrier, readily localized in brain tissue following administration, and has a strong inhibitory effect on brain tumor cells *in vitro*.<sup>18,19</sup> CAT<sub>3</sub> suppresses tumor growth by interrupting the Hedgehog signaling pathway. Additionally, CAT<sub>3</sub> blocks accumulation of the smoothened receptor and represses the transcriptional factor Gli1. The effects of CAT<sub>3</sub> on glioblastoma and medulloblastoma are now under further preclinical study.

In this study, we investigated the antitumor activity of CAT<sub>3</sub> in TMZ-resistant GBM. The active form of CAT<sub>3</sub>, PF403, was able to strongly inhibit the proliferation of U251/TMZ and T98G cells, which, respectively, represent intrinsic and acquired TMZ-resistant cells. We also demonstrated that CAT<sub>3</sub> suppressed tumor growth in the U251/TMZ orthotopic and T98G subcutaneous xenograft models at a dose of 12 mg/kg/day. In the U251/TMZ glioblastoma cells with a hyperactive Hedgehog signaling pathway and reduced MGMT expression, the antitumor effect of PF403 was mediated by disruption of the signaling pathway. Moreover, PF403 was also found to suppress T98G cells with high MGMT expression by blocking the Hedgehog signaling pathway. PF403 was able to reduce Gli1 expression, even under conditions of MGMT overexpression, in U251/TMZ cells. As a target gene of Gli1, *MGMT* expression was downregulated

by PF403 through Gli1 attenuation. Furthermore, PF403 showed good antitumor activity in combination with TMZ, and counteracted TMZ resistance both *in vitro* and *in vivo*.

## Material and methods

### Cell lines

The T98G and U251 cell lines were purchased from the American Type Culture Collection (ATCC, Manassas, VA, USA). Both T98G and U251 cells were cultured in DMEM or minimal essential medium (MEM) (Gibco, Thermo Fisher Scientific, Waltham, MA, USA) with 10% (v/v) fetal bovine serum (Gibco, Thermo Fisher Scientific) and 100 units/mL penicillin/streptomycin.

The U251/TMZ cell line was a gift from Dr Yuhui Zou of General Hospital of Guangzhou Military Command of PLA. The U251/TMZ cells were produced by repeatedly exposing U251 cells to TMZ at a single high concentration. Briefly, U251/TMZ cells were selected for a procedure consisting of 20 pulsed drug treatments with TMZ. The majority of the cells were dead following 24 hours of exposure to TMZ. The treated cells were then washed with 0.01 mol/L PBS and cultured in TMZ growth medium. After 1–2 days, the dead cells were washed with PBS and fresh TMZ medium was added. Once the cells reached 70%–80% confluence, they were preserved for further study. The TMZ-resistant cell line was stabilized for approximately 6 months after the initiation of treatment, and the resistant phenotype was developed. To maintain TMZ-resistant cells, the U251/TMZ cells were grown in the presence of 200 μM TMZ. Prior to experimentation, the U251/TMZ cells were maintained in a TMZ-free culture medium and subcultured for at least three generations. The drug-resistant characteristics of the cells were tested using various concentrations of TMZ. The experiments using the U251/TMZ cells were approved by the ethics committee for Animal Experiments of the Institute of Materia Medica, Chinese Academy of Medical Sciences & Peking Union Medical College.

### Antibodies and reagents

Anti-Smo, anti-Gli1, and anti-MGMT antibodies were purchased from Abcam (Cambridge, UK). Anti-Cyclin D1 and anti-CDK-6 antibodies were obtained from Cell Signaling Technology (Danvers, MA, USA). The anti-β-actin antibody was purchased from Santa Cruz Biotechnology Inc. (Dallas, TX, USA), and GANT61, GDC0449, and lomeguatrib were obtained from Selleck Chemicals (Houston, TX, USA). The TMZ was purchased from J&K Scientific (Beijing, People's Republic of China).

## Cell proliferation assay

The cell proliferation assay was performed using MTT (Sigma-Aldrich Co., St Louis, MO, USA). Cells were seeded in 96-well plates at various densities ( $3 \times 10^4$ /mL,  $5 \times 10^3$ /mL, and  $1.5 \times 10^3$ /mL), and treated with different compounds at various concentrations, for different intervals (24, 48, and 72 hours, respectively). The MTT solution was added to each well at the final concentration of 0.5 mg/mL. After incubation for 4 hours at 37°C, the absorbance was measured at 570 nm using a microplate reader (Biotek Instruments, Inc., Winooski, VT, USA). The IC<sub>50</sub> values were calculated using Graphpad Prism 5 Software (GraphPad Software, San Diego, CA, USA).

## Flow cytometry assay

T98G and U251/TMZ cells were cultured in six-well plates and exposed to various concentrations of PF403 for 48 hours. The cells were harvested for cell cycle or apoptosis detection via fluorescence-activated cell sorting (FACS) analysis with propidium iodide (PI)- and/or fluorescein isothiocyanate (FITC)-labeled annexin V-stained cells, according to the manufacturer's recommended procedures (Tianjin Sungene Biotech Co., Tianjin, People's Republic of China).

## MGMT overexpression

The pLenti-CMV-hMGMT plasmid was obtained from Biogot (Nanjing, Jiangsu, People's Republic of China). U251/TMZ cells were transfected with pLenti-CMV-hMGMT, using the Lipofectamine 3000 transfection reagent (Thermo Fisher Scientific) according to the manufacturer's protocols. When cells reached 80% confluence, they were treated with various concentrations of PF403 for 48 hours and harvested for immunoblotting.

## Immunoblotting analysis

Cells or tumor tissues were collected and lysed in radioimmunoprecipitation assay buffer containing 1% sodium dodecyl sulfate (SDS), 10 mmol/L ethylenediaminetetraacetic acid, 50 mmol/L Tris-HCl (pH 8.1), 1% proteinase inhibitor cocktails, and 1% protease inhibitor mixture (Sigma-Aldrich Co.). Lysates were then centrifuged at 13,000 rpm for 10 minutes, and the supernatants were collected. Protein concentrations were measured using the Micro BCA Protein Assay Kit (Thermo Fisher Scientific). Protein samples (50 µg) were separated by 12% SDS polyacrylamide gel electrophoresis and transferred to a nitrocellulose membrane using semi-wet electrophoresis. Membranes were blocked with 5% non-fat dry milk in tris-buffered saline-Tween 20

(TBS-T) and incubated overnight with primary antibodies (1:1,000 dilution) at 4°C. After being washed three times with TBS-T, the membranes were incubated with secondary antibodies (1:4,000). The immunoblots were visualized using an enhanced chemiluminescence detection kit (Pierce Biotechnology, Waltham, MA, USA) by Image Quant LAS 4000 (GE Healthcare, Little Chalfont, UK).

## Quantitative real-time PCR analysis

Total RNA was isolated using the TRIzol reagent (Biotek Co., Beijing, People's Republic of China) according to the manufacturer's recommended procedures. First-strand cDNA was synthesized from 1 µg of total RNA using the ReverTra Ace<sup>®</sup> qPCR RT Master Mix with gDNA Remover (TOYOBO, Osaka, Japan). The ABI PRISM 7900 Sequence Detection System and SYBR<sup>®</sup> Green Realtime PCR Master Mix (TOYOBO) were used to quantify gene expression. Target sequences were amplified at 95°C for 1 minute, followed by 40 cycles of 95°C for 15 seconds, 60°C for 15 seconds, and 72°C for 45 seconds. The fold changes in *Smo* and *Gli1* gene expressions were calculated according to the 2<sup>-ΔΔCt</sup> method. The primers for *Smo* and *Gli1* have been described in our previous study.<sup>18</sup>

## Orthotopic mouse tumor model and subcutaneous mouse tumor model

All animal experiments were approved by the ethics committee for Animal Experiments of the Institute of Materia Medica, Chinese Academy of Medical Sciences & Peking Union Medical College and conducted in accordance with the Guidelines of Animal Experiments. Female BALB/c athymic nude mice (Vital River Laboratories, Beijing, People's Republic of China) with body weight of 18–20 g were housed in standard specific-pathogen-free facilities. For the orthotopic tumor experiments, the procedures followed those outlined in our previous study.<sup>18</sup> Mice were anesthetized with 50 mg/kg pentobarbital sodium intraperitoneally and placed in a stereotaxic restraint. A small surgical incision was made in the skin covering the skull 2 mm to the right of the bregma. Cell suspensions (5 µL) containing approximately  $1 \times 10^6$  U251/TMZ cells were slowly (over approximately 30 seconds) injected intracranially 2.0 mm below the skull surface using a 26-gauge needle. The needle was slowly retracted after 3 minutes. The incision was immediately sutured, and 50,000 units of penicillin were injected into the mice to prevent infection. The animals were then warmed with heating mats and monitored until they regained consciousness. After 4 days, mice bearing intracranial tumors were randomized for

administration of vehicle, TMZ, and CAT<sub>3</sub> at a dose of 6 or 12 mg/kg, dissolved in 0.5% carboxymethyl cellulose (CMC) solution. Five mice were allocated to each group. The TMZ (50 mg/kg) was orally administered to mice every day for 5 days, or CAT<sub>3</sub> was orally administered once daily. For the combination study, TMZ at a dose of 50 mg/kg, and CAT<sub>3</sub> at a dose of 6 mg/kg, were each dissolved in 0.5% CMC solution. The TMZ (50 mg/kg) was orally administered to mice daily for 5 days and/or CAT<sub>3</sub> was administered once daily. An animal MRI scanner (Pharma Scan 70/16 US, Bruker Corporation, Billerica, MA, USA) was used to observe development of the intracranial tumors. The parameters for MRI were as follows: a T2\_TurboRARE, with TR/TE = 5,000/40, six averages, 20 × 20 field-of-view, and 0.5 mm slice thickness. The tumor volume based on MRI was calculated as follows:  $V = L \times W \times T$ ; where  $L$  is the maximum length of the tumor,  $W$  is the maximum width perpendicular to  $L$ , and  $T$  is the thickness of the tumor slice (0.5 mm).

For the subcutaneous mouse model, female BALB/c athymic nude mice (8–10 weeks old) were subcutaneously implanted with  $1 \times 10^7$  T98G cells in 0.1 mL Matrigel solution in the right flank. After two weeks, the tumor tissues were harvested under sterile conditions and tumor cells were extracted from the tissue homogenate. The mice were then each implanted with  $5 \times 10^6$  tumor cells. Seven days later, when the average tumor volumes reached to 100–300 mm<sup>3</sup>, the mice were randomized and received the respective treatments (Day 0). Mice were treated with orally administered TMZ (30 mg/kg or 50 mg/kg) daily for 5 days, or CAT<sub>3</sub> (6 or 12 mg/kg) once daily for 14 days. Six mice were allocated to each group. Tumor volume and body weight were monitored twice weekly. The tumor volume was calculated as follows:  $V = 1/2 \times L \times W^2$ ; where  $L$  is the maximum length of the tumor and  $W$  is the maximum width of the tumor. The mice were euthanized on day 14 and the tumor tissues were collected for immunoblotting.

## Histopathological analysis

Mouse brain or tumor samples were embedded in paraffin and 5 μm thick sections were prepared. The sections were then stained with H&E or Gli1 antibody (1:300). The stained images of each section were acquired using Olympus Confocal Microscope (FV1000 MPE; Olympus Corporation, Tokyo, Japan).

## Statistical analysis

The results were presented as mean ± standard deviation or standard error of the mean. A one-way analysis of variance

test was used to determine the statistical significance between vehicle and drug treatment groups.  $P < 0.05$  was considered to represent statistically significant differences.

## Results

### PF403 exerted potent cytotoxic activity in TMZ-resistant GBM in vitro

CAT<sub>3</sub> is a prodrug of PF403 (Figure 1A). Our previous study demonstrated that PF403 strongly inhibits proliferation of Daoy and U87MG cells.<sup>18</sup> However, it is not known whether PF403 exerts antitumor activity in TMZ-resistant glioblastoma cells. In order to investigate the putative inhibitory effect of PF403 in these cells, we employed two TMZ-resistant glioblastoma cell lines: T98G and U251/TMZ. The T98G cell line is characterized by high expression of MGMT, whereas U251/TMZ is an acquired TMZ-resistant glioblastoma cell line from U251 that barely expresses MGMT (Figure 1B). Neither of the two cell lines exhibit sensitivity to TMZ. Further, PF403-mediated cytotoxicity was detected in the two cell lines at different timepoints. The proliferation of both T98G and U251/TMZ cells was inhibited by PF403, with an IC<sub>50</sub> value of 0.004 nmol/L and 1.79 nmol/L, respectively, after 72 hours (Figure 1C; Table 1).

Next, in order to explore how PF403 inhibits tumor cell proliferation, we detected the cell cycle distribution after the exposure of U251/TMZ cells to PF403. As shown in Figure 2A, PF403 induced cell cycle arrest in the G1 phase. Consistent with flow cytometric results, cyclin D1 and cell division protein kinase 6 (CDK6), a marker of the G1 phase, both showed a decline in a dose-dependent manner (Figure 2B). Similar results were observed in T98G cells exposed to various concentrations of PF403 (Figure 2C and D). Moreover, apoptosis levels in T98G glioblastoma cells increased following exposure to PF403 over 48 hours (Figure 2E). Cleaved caspase-3 was upregulated after PF403 treatment, whereas levels of full-length poly ADP ribose polymerase and Bcl-2 were reduced (Figure 2F). However, apoptosis was not detected in U251/TMZ cells treated with PF403 for 48 hours. These data suggest that PF403 exerted a strong proliferative inhibition on TMZ-resistant GBM cells in vitro.

### PF403 suppressed TMZ-resistant GBM cells via the Hedgehog-signaling pathway, independently of MGMT expression

In our previous study, we demonstrated that PF403 suppressed glioblastoma and medulloblastoma by interrupting the Hedgehog signaling pathway.<sup>18</sup> Thus, to elucidate whether

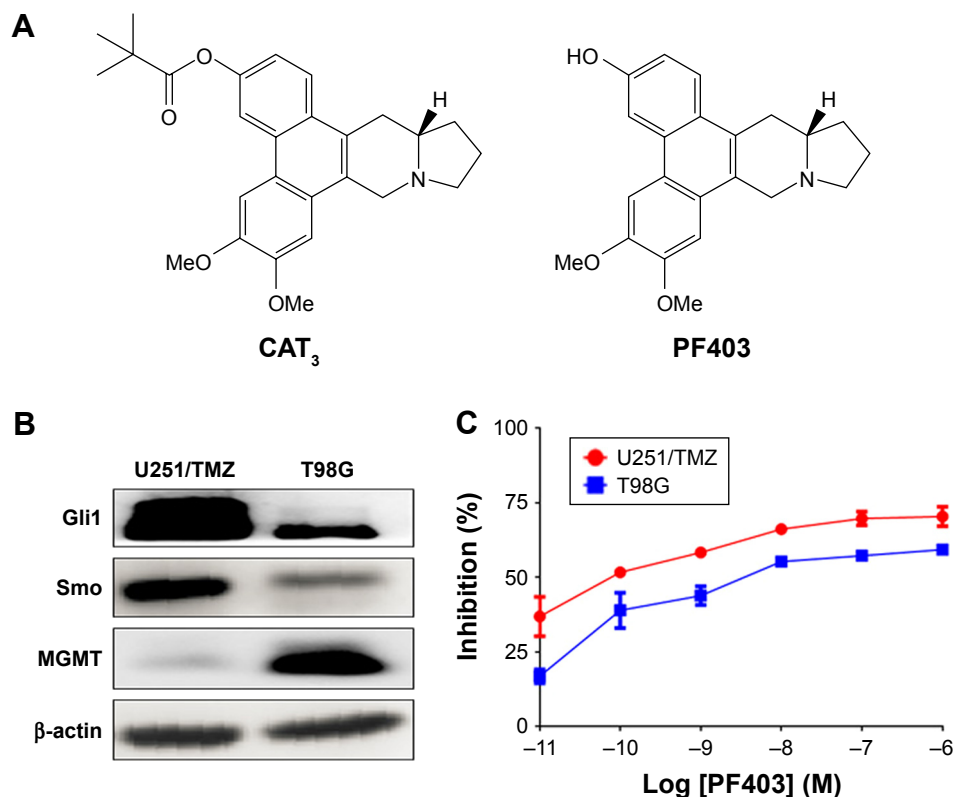


**Figure 1** PF403 inhibited the proliferation of TMZ-resistant GBM cells. **(A)** Chemical structure of CAT<sub>3</sub> and its active metabolite, PF403. **(B)** Protein expression levels of Gli1, Smo, and MGMT in TMZ-resistant GBM cells, U251/TMZ, and T98G. **(C)** Cell proliferative inhibition curve of U251/TMZ and T98G treated for 72 hours with various concentrations of PF403.

**Abbreviations:** GBM, glioblastoma multiforme; MGMT, O<sup>6</sup>-methylguanine DNA methyltransferase; PF403, 13a(S)-3-hydroxyl-6,7-dimethoxyphenanthro[9,10-b]-indolizidine; Smo, smoothened; TMZ, temozolomide.

PF403 also suppresses TMZ-resistant glioblastoma cells via the Hedgehog signaling pathway, we first assessed the effects of PF403 on the key factors of this pathway, specifically the protein and mRNA levels of Smo and Gli1. Immunoblotting results indicated that PF403 reduced protein levels of Smo and Gli1 in a dose-dependent manner (Figure 3A). Similar results have been observed in the positive control, GDC0449, which is reportedly a Hedgehog inhibitor.<sup>6</sup> In addition, PF403 downregulated the expression of *Smo* and *Gli1* mRNA (Figure 3B). As the target genes of Gli1, the

expression of cyclin D1 and cyclin D2 was suppressed by PF403 (Figure 3C). When stimulated by Shh, PF403 blocked the action of Shh on Gli1 (Figure 3D). These data indicate that PF403 exhibited considerable antitumor activity in U251/TMZ via inhibition of the Hedgehog signaling pathway.

Furthermore, we explored whether PF403 blocked the Hedgehog signaling pathway in T98G cells, in which MGMT was highly expressed. Protein levels of both Gli1 and Smo showed a decline in response to different doses of PF403 (Figure 4A). Surprisingly, MGMT expression was also attenuated after PF403 treatment in a dose-dependent manner. Therefore, we assumed that PF403 inhibits T98G cell proliferation through both the Hedgehog pathway and MGMT. Cell proliferation was detected in T98G cells exposed to PF403 in combination with lomeguatrib, an MGMT inhibitor. In comparison with PF403 treatment alone, lomeguatrib did not enhance proliferative inhibition in the combination group (Figure 4B); whereas the antiproliferative effect was increased following TMZ treatment together with lomeguatrib (Figure 4C and D). Previous reports identify MGMT as the target gene of Gli1.<sup>20</sup> Thus, after the

**Table 1** PF403- and TMZ-mediated inhibition of proliferation in TMZ-resistant glioblastoma cells

Time (hours)	IC <sub>50</sub> (mol/L)			
	U251/TMZ		T98G	
	PF403	TMZ	PF403	TMZ
24	3.20 ± 0.64 × 10 <sup>-5</sup>	>1 × 10 <sup>-3</sup>	3.47 ± 1.24 × 10 <sup>-5</sup>	>1 × 10 <sup>-3</sup>
48	2.73 ± 1.37 × 10 <sup>-8</sup>	>1 × 10 <sup>-3</sup>	1.49 ± 0.95 × 10 <sup>-6</sup>	>1 × 10 <sup>-3</sup>
72	4.14 ± 1.08 × 10 <sup>-12</sup>	>1 × 10 <sup>-3</sup>	1.79 ± 0.82 × 10 <sup>-9</sup>	>1 × 10 <sup>-3</sup>

**Note:** Data are presented as mean ± standard deviation.

**Abbreviations:** IC<sub>50</sub>, half maximal inhibitory concentration; PF403, 13a(S)-3-hydroxyl-6,7-dimethoxyphenanthro[9,10-b]-indolizidine; TMZ, temozolomide.

Hedgehog signaling pathway was activated by Shh, protein levels of both Gli1 and MGMT were elevated, whereas PF403 blocked the effects of Shh (Figure 4E). Furthermore, MGMT was overexpressed in U251/TMZ cells and Gli1 was still downregulated in a dose-dependent manner after treatment with PF403. Cyclin D1, as a positive control and a Gli1 target gene, was also reduced after treatment (Figure 4F). Considered together, these findings indicate that PF403 suppresses TMZ-resistant glioblastoma cells via the Hedgehog signaling pathway, independently of MGMT status.

### CAT<sub>3</sub> inhibited TMZ-resistant glioblastoma growth in vivo

After confirming antitumor activity of PF403 in vitro, we further investigated whether CAT<sub>3</sub>, a prodrug of PF403, inhibits tumor growth in the TMZ-resistant glioblastoma xenograft model. The U251/TMZ orthotopic model was employed to evaluate the antitumor effect of CAT<sub>3</sub>. In comparison with the vehicle group, the tumor volumes in the CAT<sub>3</sub> group were significantly reduced at a dose of 12 mg/kg with *P*-value less than 0.05 (Figure 5A and B). These findings indicate that the

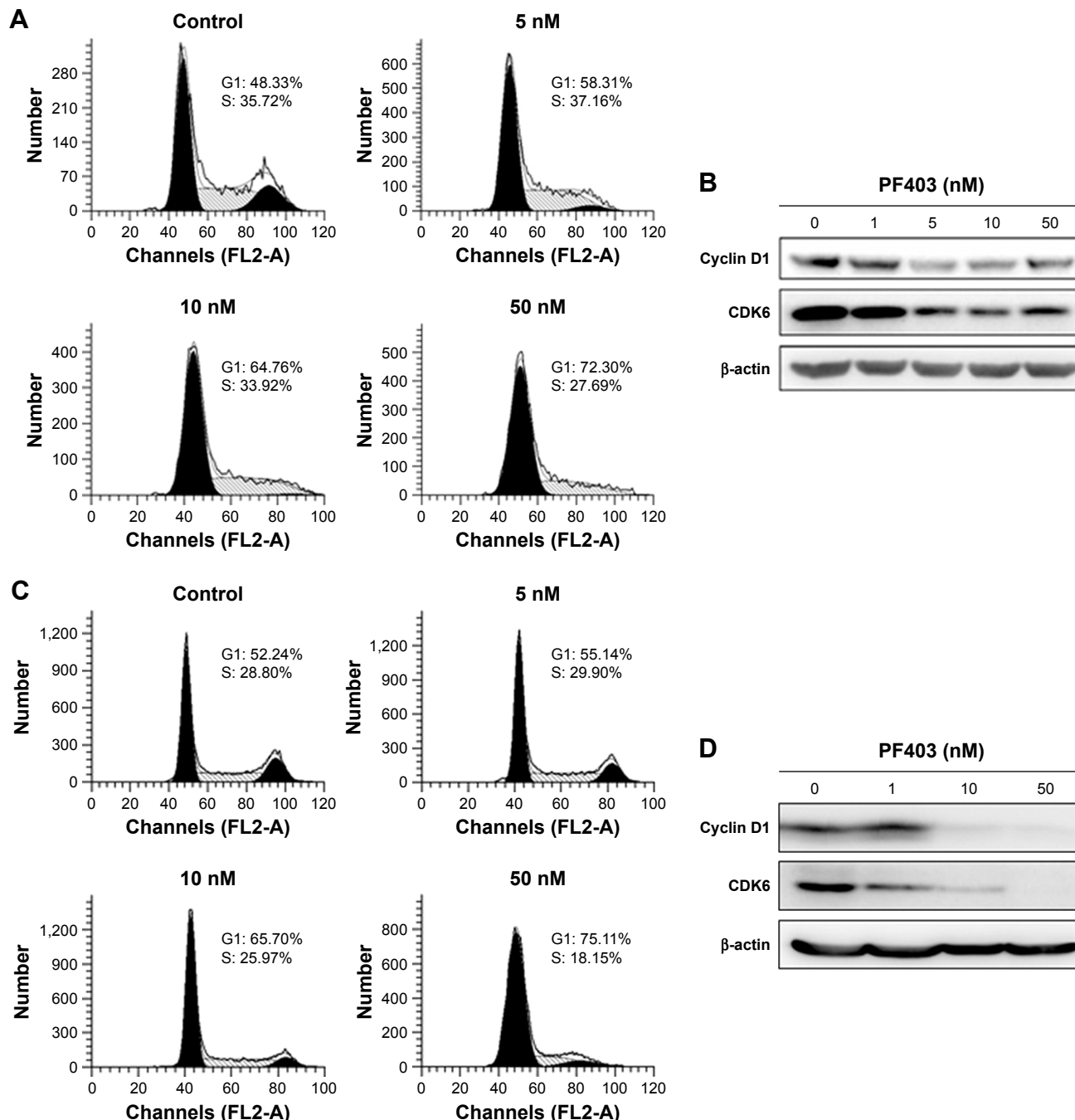
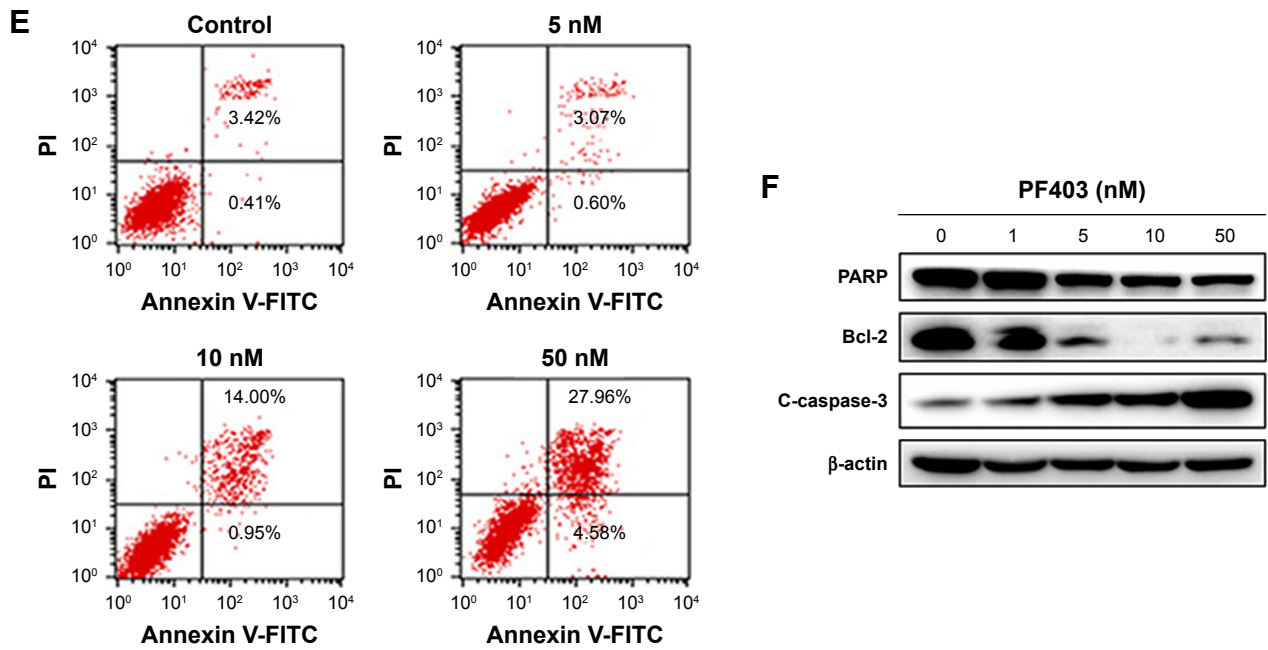
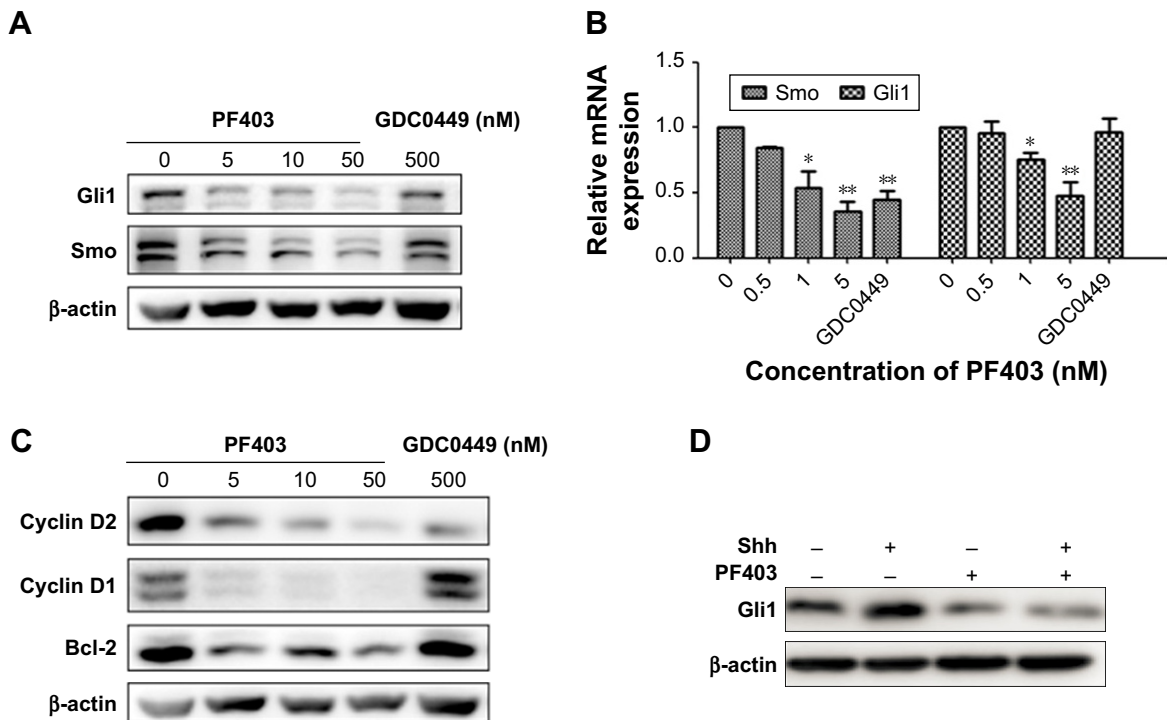


Figure 2 (Continued)



**Figure 2** PF403-induced cell cycle arrest and apoptosis in GBM cells. (A) Exposure to various concentrations of PF403 for 48 hours; U251/TMZ cells were stained with PI for flow cytometry analysis. (B) Protein levels of cyclin D1 and CDK6 were detected via immunoblotting, following the exposure of U251/TMZ cells to PF403 for 48 hours. (C) Exposure to various concentrations of PF403 for 48 hours; T98G cells were stained with PI for flow cytometry analysis. (D) Protein levels of cyclin D1 and CDK6 were detected via immunoblotting, following exposure of T98G cells to PF403 for 48 hours. (E) Exposure to various concentrations of PF403 for 48 hours; T98G cells were stained with annexin V-FITC and PI for flow cytometry analysis. (F) Protein levels of full length PARP, Bcl-2, and cleaved caspase-3 were detected via immunoblotting in T98G cells, following exposure to PF403 for 48 hours.

**Abbreviations:** CDK6, cell division protein kinase 6; FITC, fluorescein isothiocyanate; GBM, glioblastoma multiforme; PARP, poly ADP ribose polymerase; PF403, 13a(S)-3-hydroxyl-6,7-dimethoxyphenanthro[9,10-b]-indolizidine; PI, propidium iodide; TMZ, temozolomide.



**Figure 3** PF403 repressed the Hedgehog signaling pathway in U251/TMZ cells. (A) Protein levels of Gli1 and Smo were detected via immunoblotting in U251/TMZ cells exposed to various concentrations of PF403 or GDC0449 for 48 hours. (B) The mRNA levels of Gli1 and Smo were detected via real-time PCR in U251/TMZ cells exposed to PF403 for 48 h. \* $P < 0.05$  and \*\* $P < 0.01$  compared to control group. (C) Protein levels of cyclin D1, cyclin D2, and Bcl-2 were detected via immunoblotting in U251/TMZ cells exposed to PF403 for 48 hours. (D) U251/TMZ cells were pretreated with PF403 (5 nM) for 1 hour, following the addition of recombinant Shh (500 ng/mL) over 48 hours. Protein levels of Gli1 were detected via immunoblotting.

**Abbreviations:** PCR, polymerase chain reaction; PF403, 13a(S)-3-hydroxyl-6,7-dimethoxyphenanthro[9,10-b]-indolizidine; Shh, sonic Hedgehog; Smo, smoothened; TMZ, temozolomide.

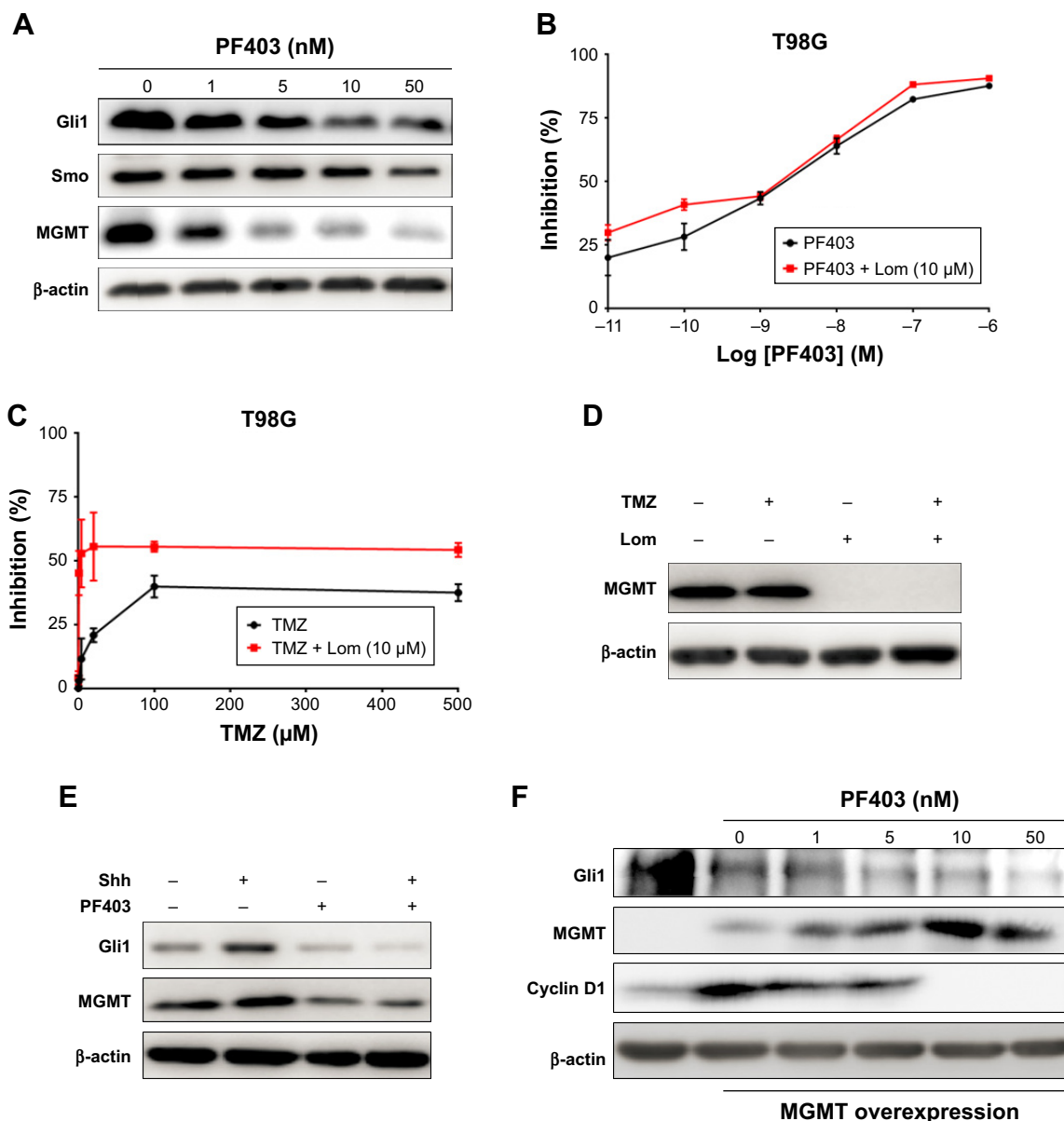


**Figure 4** PF403 blocked the Hedgehog signaling pathway in T98G cells and downregulated MGMT expression. **(A)** Protein levels of Gli1, Smo, and MGMT were detected via immunoblotting in T98G cells exposed to various concentrations of PF403 for 48 hours. **(B)** Cell inhibition curve of T98G cells treated with various concentrations of PF403 alone or in combination with Lom for 72 hours. **(C)** Cell inhibition curve of T98G cells treated with various concentrations of TMZ alone, or in combination with Lom for 72 hours. **(D)** T98G cells were pretreated with Lom (10 μM) for 1 hour, following the addition of TMZ (250 μM) over 48 hours. Protein levels of MGMT were detected via immunoblotting. **(E)** T98G cells were pretreated with PF403 (5 nM) for 1 hour, following the addition of Shh (500 ng/mL) over 48 hours. Protein levels of Gli1 and MGMT were detected via immunoblotting. **(F)** U251/TMZ cells were transfected with pLenti-CMV-hMGMT and treated with various concentrations of PF403. Protein levels of Gli1, MGMT, and cyclin D1 were detected via immunoblotting.

**Abbreviations:** Lom, lomeguatrib; MGMT, O<sup>6</sup>-methylguanine DNA methyltransferase; PF403, 13a(S)-3-hydroxyl-6,7-dimethoxyphenanthro[9,10-b]-indolizidine; Shh, sonic Hedgehog; Smo, smoothened; TMZ, temozolomide.

TMZ treatment was not effective in U251/TMZ orthotopic model. Histological analysis of the mice brains indicated that PF403 effectively inhibited tumor invasion and downregulated Gli1 in tumor issue (Figure 5C).

Furthermore, we investigated whether CAT<sub>3</sub> additionally inhibits the growth of T98G glioblastoma with high MGMT expression in a xenograft model. As shown in Figure 5D and E, CAT<sub>3</sub> exerted far more effective tumor

growth-inhibitory effects, particularly at a dose of 12 mg/kg, in comparison with TMZ at either dose of 30 mg/kg or 50 mg/kg. The immunoblotting results of the tumor issues indicated that Gli1, Smo, and MGMT were all inhibited after CAT<sub>3</sub> treatment (Figure 5F). Histological results showed that PF403 reduced Gli1 levels in tumor issues (Figure 5G). These results indicate that CAT<sub>3</sub> exhibited antitumor activity in TMZ-resistant GBM in vivo.



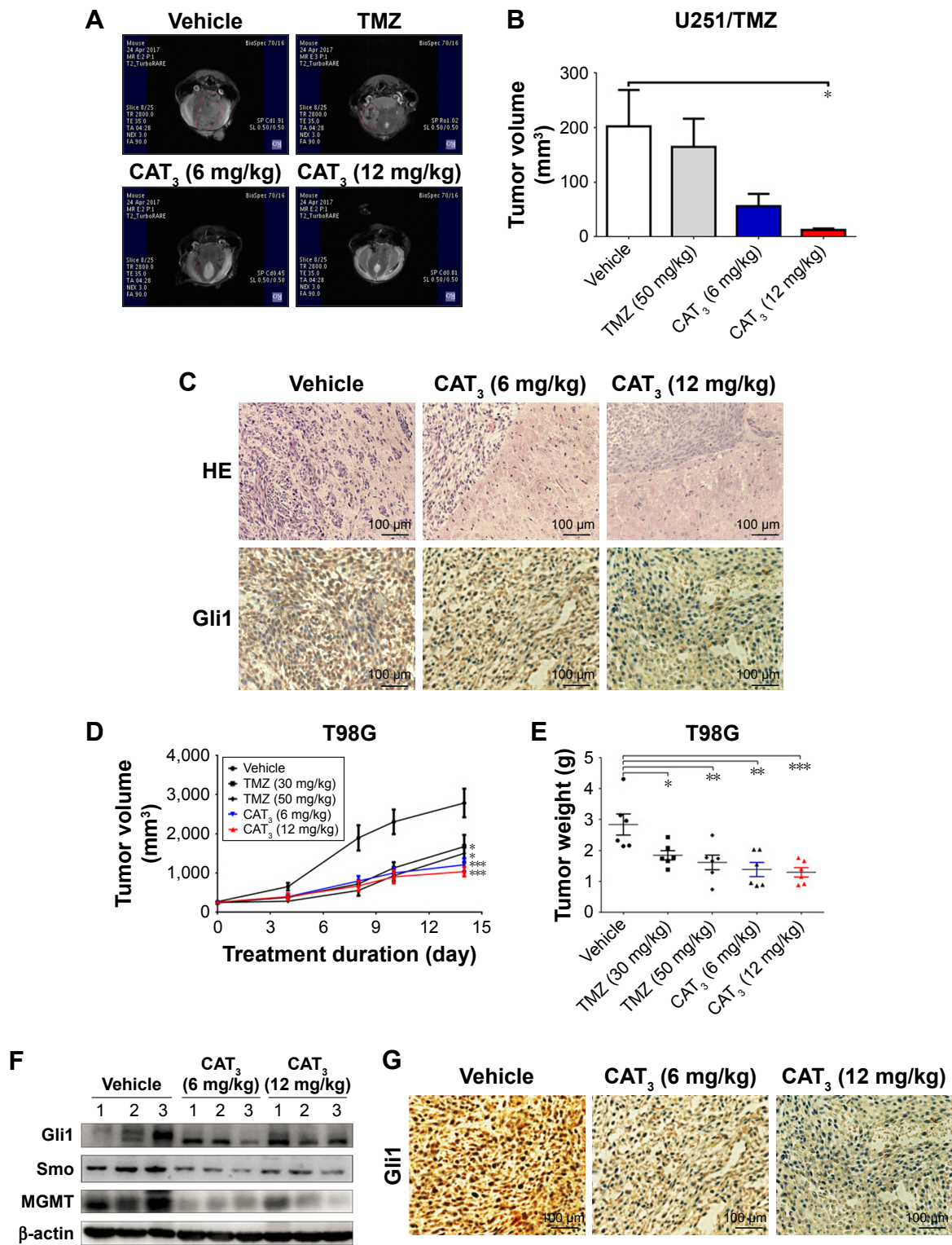


**Figure 5** CAT<sub>3</sub>-inhibited tumor growth of TMZ-resistant GBM in vivo. **(A)** MRI T2-weighted image of intracranial tumors from various groups of the U251/TMZ orthotopic model. TMZ (50 mg/kg) was orally administered to mice for 5 days or CAT<sub>3</sub> was administered daily. **(B)** Tumor volumes in the U251/TMZ orthotopic model. \**P* < 0.05, compared to the vehicle group, ANOVA analysis. **(C)** Histological analysis of tumor tissues in the mouse brain of the U251/TMZ orthotopic model. H&E staining (200×), Gli1 staining (200×). **(D)** Tumor growth curve in T98G subcutaneous xenograft model. TMZ was orally administered (30 mg/kg or 50 mg/kg) to mice for 5 days or CAT<sub>3</sub> was administered daily. \**P* < 0.05 and \*\*\**P* < 0.001, compared to the vehicle group, ANOVA analysis. **(E)** Tumor weight in individual mice in the T98G subcutaneous xenograft model. \**P* < 0.05, \*\**P* < 0.01, and \*\*\**P* < 0.001, compared to the vehicle group, ANOVA analysis. **(F)** Tumor tissues from the T98G subcutaneous xenograft model were collected and Gli1, Smo, and MGMT levels were detected via immunoblotting. **(G)** Histological analysis of tumor tissues in the T98G subcutaneous xenograft model. Gli1 staining (200×).

**Abbreviations:** ANOVA, analysis of variance; GBM, glioblastoma multiforme; H&E, hematoxylin and eosin; MGMT, O<sup>6</sup>-methylguanine DNA methyltransferase; Smo, smoothened; TMZ, temozolomide.

# CAT<sub>3</sub> enhanced antitumor activity of TMZ in TMZ-resistant glioblastoma

The Hedgehog signaling pathway is reportedly also involved in TMZ resistance.<sup>20</sup> Disruption of the Hedgehog signaling pathway by Gli1 improves the sensitivity of GBM to TMZ.<sup>21</sup> We first examined the inhibitory effects of TMZ after

blockade of the Hedgehog signaling pathway with PF403 in U251/TMZ and T98G cells. After incubation for 72 hours, PF403 was found to enhance the antiproliferative effect of TMZ. As the positive control, the Gli-specific inhibitor, GANT61, also acted synergistically with TMZ (Figure 6A and B). As shown in Figure 6C, the protein level of Gli1 was

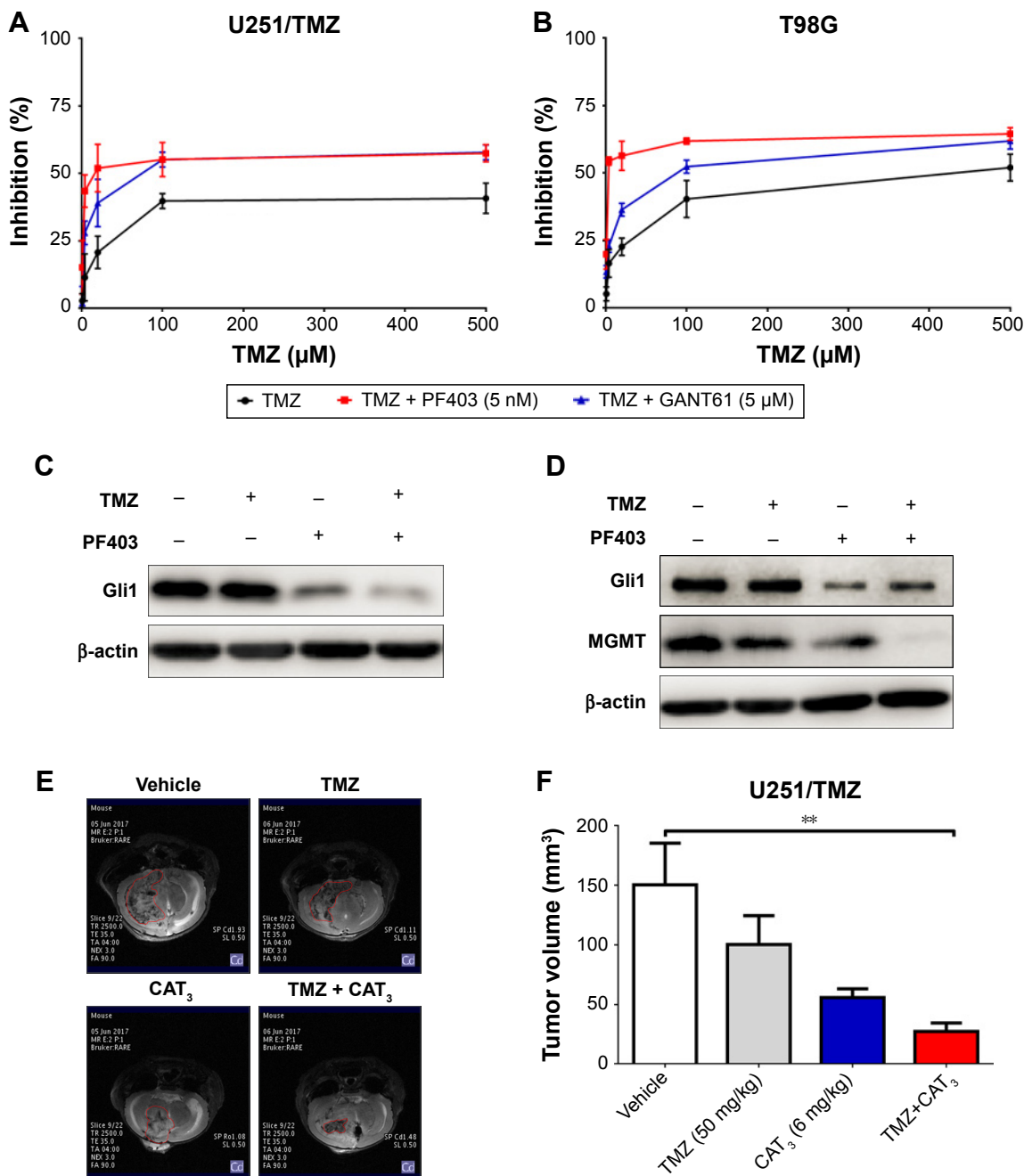


**Figure 6** CAT<sub>3</sub> enhanced antitumor activity of TMZ in TMZ-resistant GBM. (A, B) Cell proliferation inhibition curve of U251/TMZ and T98G cells treated with various concentrations of TMZ alone, or in combination with PF403 (5 nmol/L) or GANT61 (5 μmol/L) for 72 hours. (C) U251/TMZ cells were pretreated with PF403 (5 nM) for 1 h, following the addition of TMZ (250 μmol/L) over 48 hours. Protein levels of Gli1 were detected via immunoblotting. (D) T98G cells were pretreated with PF403 (5 nmol/L) for 1 hour, following the addition of TMZ (250 μmol/L) over 48 hours. Protein levels of Gli1 and MGMT were detected via immunoblotting. (E) MRI T2-weighted image of intracranial tumors from various groups of the U251/TMZ orthotopic model. TMZ was orally administered (50 mg/kg) to mice for 5 days; or CAT<sub>3</sub> (6 mg/kg) was orally administered daily; or a combination (TMZ 50 mg/kg for 5 days + CAT<sub>3</sub> 6 mg/kg daily). (F) Tumor volumes in the U251/TMZ orthotopic mouse model. \*\*P < 0.01, compared to the vehicle group, ANOVA analysis.

**Abbreviations:** ANOVA, analysis of variance; GBM, glioblastoma multiforme; MGMT, O<sup>6</sup>-methylguanine DNA methyltransferase; TMZ, temozolomide.

not altered by TMZ; the effects of their combination could be attributed to the downregulation of Gli1 by PF403. Consistent results were observed in T98G cells (Figure 6D). As the target gene of Gli1, *MGMT* was also downregulated by PF403.

We conducted another animal study using the U251/TMZ orthotopic model to investigate the efficacy of the combination of TMZ and CAT<sub>3</sub>. As shown in Figure 6E and F, both TMZ and CAT<sub>3</sub> monotherapies were not able to reduce tumor size with statistical difference. The tumors in the group treated with a combination of TMZ and CAT<sub>3</sub> showed a trend toward greatest reduction of tumor volume. These data indicate that the Hedgehog signaling pathway plays an important role in TMZ resistance in glioblastoma cells, and that CAT<sub>3</sub> counteracts TMZ resistance via this pathway.

## Discussion

As a malignant high-grade glioma, GBM is refractory to chemotherapy and radiotherapy and is characterized by a poor clinical outcome. TMZ remains the first choice for treatment.<sup>10</sup> However, the efficacy of TMZ during clinical treatment is limited by the development of TMZ resistance, necessitating the development of novel agents for GBM therapy. In our previous work, we found that CAT<sub>3</sub> exhibited strong antitumor activity in medulloblastoma and glioblastoma.<sup>18</sup> However, the efficacy of CAT<sub>3</sub> in TMZ-resistant GBM remains unclear. Here, we tested the antitumor activity of CAT<sub>3</sub> in TMZ-resistant GBM.

Amplification of *EGFR*; mutation of *PIK3CA*, *IDH1*, and *EGFRvIII*; and aberrations in the Hedgehog signaling pathway have all been identified as triggers of GBM development.<sup>2-4</sup> Novel approaches to GBM treatment involve targeting these factors. Inhibition of the Hedgehog signaling pathway has been shown to exert antitumor activity in GBM. Sonidegib, a Hedgehog pathway inhibitor, represses tumor growth in an orthotopic Ptc<sup>+/-</sup>p53<sup>-/-</sup> medulloblastoma allograft model.<sup>22</sup> Furthermore, CAT<sub>3</sub> inhibits tumor growth by disrupting the Hedgehog signaling pathway.<sup>18</sup> In this study, we employed two different types of glioblastoma cells that are resistant to TMZ: U251/TMZ cells are acquired TMZ-resistant cells that grow faster than U251 cells, in which Gli1 is highly expressed (Figure S1); whereas T98G cells are intrinsic TMZ-resistant cells. We evaluated the proliferative inhibition of TMZ in these two cell lines. In comparison with U251, TMZ was not effective in U251/TMZ cells (Tables 1 and S1). For T98G cells, the IC<sub>50</sub> value of TMZ over 72 hours was much greater than 1 mM, which is the consistent value in previously published data.<sup>13</sup> In such TMZ-resistant cell lines, PF403 induces both U251/TMZ and T98G cell cycle arrest in the G1 phase. Thus, PF403 was able to induce T98G apoptosis;

however, apoptosis was not observed in U251/TMZ cells after exposure to PF403 over 48 hours. This might be due to the various concentrations and duration of treatment.

We also found that CAT<sub>3</sub> inhibited the proliferation of both cell lines in vitro, and repressed tumor growth in vivo. The antitumor activity of CAT<sub>3</sub> in TMZ-resistant glioblastoma could be attributed to disruption of the Hedgehog signaling pathway, and downregulation Gli1 and Smo. Moreover, PF403 antagonizes the effects of Shh on activation of the Hedgehog signaling pathway. In addition, the toxicity of CAT<sub>3</sub> was acceptable. No noticeable effects of PF403 were observed on the proliferation of HK2 and H9C2 cells, and its inhibitory effect on PC12 cells was comparatively weaker (Figures S2 and S3). No significant differences in body weight were observed between CAT<sub>3</sub> treatment groups and the vehicle group (Figure S4).

Numerous factors, including *MGMT*, Gli, and p-glycoprotein play a role in TMZ resistance. As disruption of the Hedgehog signaling pathway sensitizes glioma cells to TMZ treatment,<sup>21</sup> it is conceivable that inhibition of Gli counteracts TMZ resistance. Indeed, when combined with PF403, the activity of TMZ was enhanced in U251/TMZ cells. Similar results were observed for GANT61, a Gli inhibitor. The activity of the combination treatment was also observed in the U251/TMZ orthotopic mouse model. By blocking the Hedgehog signaling pathway, PF403 overcomes TMZ resistance.

Another key factor that induces TMZ resistance is *MGMT*. The expression pattern of *MGMT*, including the methylation status of the promoter, is a predictor of the clinical outcome of GBM.<sup>14</sup> The Hedgehog signaling pathway reportedly regulates *MGMT* expression and chemoresistance to TMZ in human glioblastoma.<sup>20,21</sup> In the present study, U251/TMZ (low *MGMT* expression) and T98G (high *MGMT* expression) reflected differences in *MGMT* expression. We found that, in the TMZ-resistant glioblastoma with high *MGMT* expression, attenuation of Hedgehog signaling by PF403 also resulted in downregulation of *MGMT* protein expression. We were unable to detect *MGMT* by immunoblotting after PF403 treatment, owing to low expression of *MGMT* in U251/TMZ cells. Furthermore, PF403 reduced Gli1 expression even when *MGMT* was overexpressed in U251/TMZ. Thus, the antitumor activity of PF403 is independent of *MGMT* expression.

## Conclusion

Our study demonstrated that CAT<sub>3</sub> exhibited antitumor activity via blockade of the Hedgehog pathway and enhanced TMZ cytotoxicity in TMZ-resistant GBM.

## Acknowledgment

This work was financially supported by the CAMS Initiative for Innovative Medicine (No. 2016-I2M-1-010), PUMC Youth Fund (No. 2017350006), and PUMC Graduate Innovation Fund (No. 2017-1007-03).

## Disclosure

The authors report no conflicts of interest in this work.

## References

- Aliferis C, Trafalis DT. Glioblastoma multiforme: pathogenesis and treatment. *Pharmacol Ther.* 2015;152:63–82.
- Brennan CW, Verhaak RG, McKenna A, et al. The somatic genomic landscape of glioblastoma. *Cell.* 2013;155(2):462–477.
- Cancer Genome Atlas Research Network. Comprehensive genomic characterization defines human glioblastoma genes and core pathways. *Nature.* 2008;455(7216):1061–1068.
- Louis DN. Molecular pathology of malignant gliomas. *Annu Rev Pathol.* 2006;1:97–117.
- Smelkinson MG. The Hedgehog signaling pathway emerges as a pathogenic target. *J Dev Biol.* 2017;5(4). doi:10.3390/jdb5040014.
- Proctor AE, Thompson LA, O'Bryant CL. Vismodegib: an inhibitor of the Hedgehog signaling pathway in the treatment of basal cell carcinoma. *Ann Pharmacother.* 2014;48(1):99–106.
- Danhof R, Lewis K, Brown M. Small molecule inhibitors of the Hedgehog pathway in the treatment of basal cell carcinoma of the skin. *Am J Clin Dermatol.* 2018;19(2):195–207.
- Braun S, Oppermann H, Mueller A, et al. Hedgehog signaling in glioblastoma multiforme. *Cancer Biol Ther.* 2012;13(7):487–495.
- Skoda AM, Simovic D, Karin V, et al. The role of the Hedgehog signaling pathway in cancer: a comprehensive review. *Bosn J Basic Med Sci.* 2018;18(1):8–20.
- National Comprehensive Cancer Network (NCCN). Clinical practice guidelines in oncology: central nervous system cancers (2017.V1). Available from: [https://www.nccn.org/professionals/physician\\_gls/default.aspx](https://www.nccn.org/professionals/physician_gls/default.aspx). Accessed January 18, 2018.
- Kitange GJ, Carlson BL, Schroeder MA, et al. Induction of MGMT expression is associated with temozolomide resistance in glioblastoma xenografts. *Neuro Oncol.* 2009;11(3):281–291.
- Johannessen TC, Bjerkvig R. Molecular mechanisms of temozolomide resistance in glioblastoma multiforme. *Expert Rev Anticancer Ther.* 2012;12(5):635–642.
- Lee SY. Temozolomide resistance in glioblastoma multiforme. *Genes Dis.* 2016;3(3):198–210.
- Hegi ME, Diserens AC, Gorlia T, et al. MGMT gene silencing and benefit from temozolomide in glioblastoma. *N Engl J Med.* 2005;352(10):997–1003.
- Thon N, Kreth S, Kreth FW. Personalized treatment strategies in glioblastoma: MGMT promoter methylation status. *Onco Targets Ther.* 2013;6:1363–1372.
- Hegi ME, Diserens AC, Godard S, et al. Clinical trial substantiates the predictive value of O-6-methylguanine-DNA methyltransferase promoter methylation in glioblastoma patients treated with temozolomide. *Clin Cancer Res.* 2004;10(6):1871–1874.
- Liu Z, Lv H, Li H, et al. Interaction studies of an anticancer alkaloid, (+)-(13aS)-deoxytylophorinine, with calf thymus DNA and four repeated double-helical DNAs. *Chemotherapy.* 2011;57(4):310–320.
- Chen J, Lv H, Hu J, et al. CAT3, a novel agent for medulloblastoma and glioblastoma treatment, inhibits tumor growth by disrupting the Hedgehog signaling pathway. *Cancer Lett.* 2016;381(2):391–403.
- Li C, Li Y, Lv H, et al. The novel anti-neuroblastoma agent PF403, inhibits proliferation and invasion in vitro and in brain xenografts. *Int J Oncol.* 2015;47(1):179–187.
- Wang K, Chen D, Qian Z, Cui D, Gao L, Lou M. Hedgehog/Gli1 signaling pathway regulates MGMT expression and chemoresistance to temozolomide in human glioblastoma. *Cancer Cell Int.* 2017;17:117.
- Li J, Cai J, Zhao S, et al. GANT61, a GLI inhibitor, sensitizes glioma cells to the temozolomide treatment. *J Exp Clin Cancer Res.* 2016;35(1):184.
- Pan S, Wu X, Jiang J, et al. Discovery of NVP-LDE225, a potent and selective smoothened antagonist. *ACS Med Chem Lett.* 2010;1(3):130–134.

## Supplementary materials

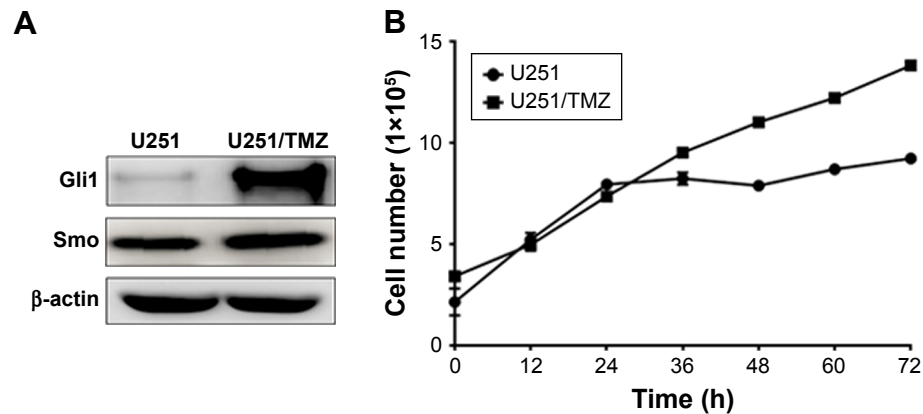


**Figure S1** Characteristics of U251 and U251/TMZ cells. **(A)** Protein expression levels of Gli1 and Smo in U251 and U251/TMZ cells. **(B)** Cell growth curve of U251 and U251/TMZ cells. The cell number was directly monitored and calculated using the HoloMonitor M4 incubator cytometer and microscope.

**Abbreviations:** Smo, smoothened; TMZ, temozolomide.

**Table S1** Inhibition of proliferation of U251 cells by PF403 and TMZ

Compounds	IC <sub>50</sub> (mol/L)
PF403	$5.36 \pm 1.18 \times 10^{-11}$
TMZ	$6.74 \pm 0.83 \times 10^{-4}$

**Notes:** U251 cells were treated with various concentrations of PF403 and TMZ for 72 hours. Data are presented as mean  $\pm$  standard deviation.

**Abbreviations:** IC<sub>50</sub>, half maximal inhibitory concentration; PF403, 13a(S)-3-hydroxyl-6,7-dimethoxyphenanthro[9,10-b]-indolizidine; TMZ, temozolomide.

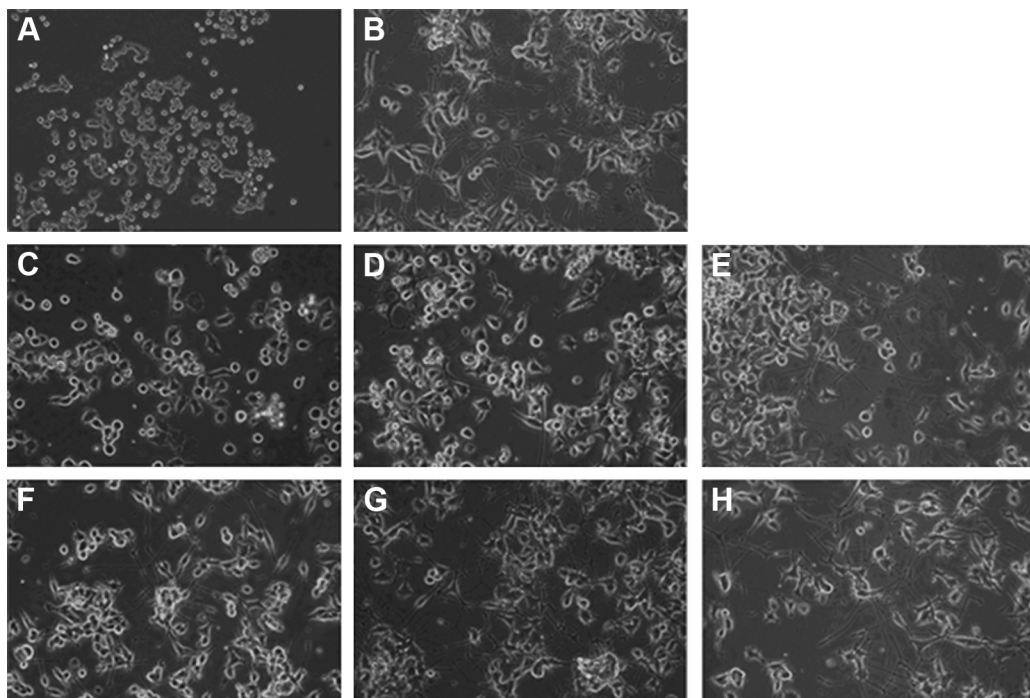


**Figure S2** Effects of PF403 on the development of synapses in rat neuronal PC12 cells. **(A)** PC12 cells without NGF treatment. **(B)** PC12 cells with NGF treatment. **(C–E)** NGF-induced PC12 cells with vincristine pretreatment ( $10^{-7}$ ,  $10^{-8}$ , and  $10^{-9}$  mol/L). **(F–H)** NGF-induced PC12 cells with PF403 pretreatment ( $10^{-7}$ ,  $10^{-8}$ , and  $10^{-9}$  mol/L). Magnification  $\times 200$ .

**Abbreviations:** NGF, nerve growth factor; PF403, 13a(S)-3-hydroxyl-6,7-dimethoxyphenanthro[9,10-b]-indolizidine.

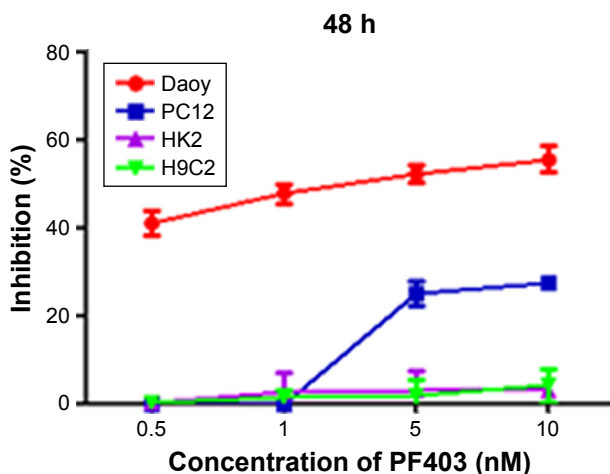


**Figure S3** Effects of PF403 on the proliferation of tumor cells and normal cells. Cells were treated with various concentrations of PF403 for 48 hours and were then subjected to the MTT assay. Daoy represents the human medulloblastoma cell line. PC12 represents rat neuronal cells. HK2 and H9C2 cells represent human kidney cells and rat cardiomyocytes, respectively.

**Abbreviations:** MTT, 3-(4,5-dimethylthiazole-2-yl)-2,5-diphenyltetrazolium bromide; PF403, 13a(S)-3-hydroxyl-6,7-dimethoxyphenanthro[9,10-b]-indolizidine.

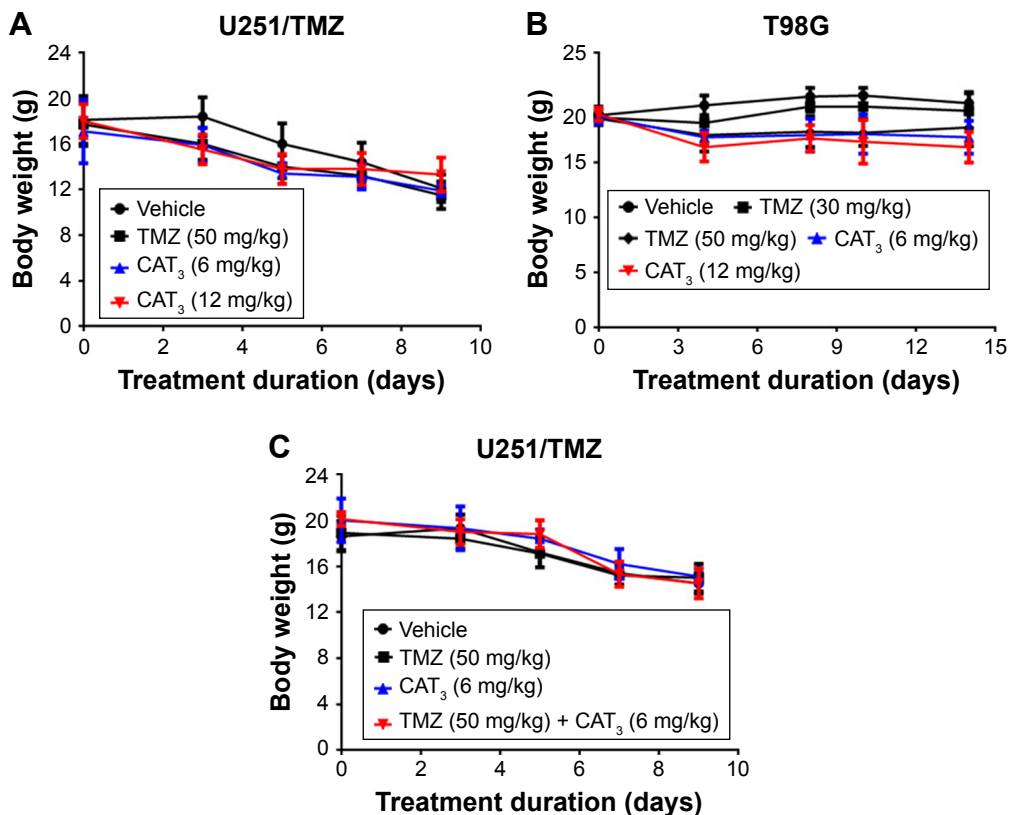


**Figure S4** Body weight curve for mice xenograft models. (A) Body weight curve for the U251/TMZ orthotopic model. (B) Body weight curve for the T98G subcutaneous xenograft model. (C) Body weight curve for the U251/TMZ orthotopic model (combination).

**Abbreviation:** TMZ, temozolomide.

OncoTargets and Therapy



Publish your work in this journal

OncoTargets and Therapy is an international, peer-reviewed, open access journal focusing on the pathological basis of all cancers, potential targets for therapy and treatment protocols employed to improve the management of cancer patients. The journal also focuses on the impact of management programs and new therapeutic agents and protocols on

patient perspectives such as quality of life, adherence and satisfaction. The manuscript management system is completely online and includes a very quick and fair peer-review system, which is all easy to use. Visit <http://www.dovepress.com/testimonials.php> to read real quotes from published authors.

Submit your manuscript here: <http://www.dovepress.com/oncotargets-and-therapy-journal>